Available online at www.sciencedirect.com
ScienceDirect
Cement & Concrete Composites 29 (2007) 566–574
Cement & Concrete Composites
www.elsevier.com/locate/cemconcomp

Failure mechanism of normal and high-strength concrete with rice-husk ash

Graciela Giaccio [a], Gemma Rodríguez de Sensale [b,*], Raúl Zerbino [a]

[a] *LEMIT-CIC, 52 e/121 y 122, 1900 La Plata, Argentina*
[b] *Facultad de Ingeniería, Julio Herrera y Reissig 565, CP 11300, Montevideo, Uruguay*

Received 20 May 2006; received in revised form 10 April 2007; accepted 11 April 2007
Available online 18 April 2007

Abstract

Mineral admixtures generally lead to a densification of the concrete internal structure. In this sense, the failure mechanism could be modified so that the concrete exhibits a more brittle behaviour. This paper discusses the effects of rice-husk ash (RHA) additions to concrete, based on analyses of the mechanical behaviour of normal and high-strength concrete. The stress–strain response in compression and load vs. CMOD (or deflection) in bending were analysed. It appears that the incorporation of RHA in concrete increases the strength, particularly for lower water/binder ratio concretes. The analysis of the failure mechanism indicates a tendency for more brittle failure behaviour in RHA concretes. For the same strength level, however, the energy of fracture was reduced no more than 10%, which is much smaller than the variations that may be produced by a change in the type or size of coarse aggregate.

Keywords: Rice-husk ash; Fracture; Fracture energy; Strength; Failure mechanism; Stiffness

1. Introduction

Concretes with compressive strength higher than 50 MPa are usually defined as high-strength concrete (HSC), according ACI Committee 363 [1]. The potential advantages of HSC extend beyond strength to include improvements in durability and service life of concrete structures.

High-strength concretes (HSC) are characterized by a low porosity and show an internal structure more uniform at the matrix–aggregate interface than normal strength concretes (NSC). Strong interfaces enhance the strength and stiffness, although such concrete usually shows more brittle behaviour [2–5]. The effects of strength level and aggregate type on the failure mechanism of NSC and HSC have been previously discussed [6–11].

Over the past years, there has been an increase in the use of industrial, agricultural and thermoelectric plant residues in the production of concrete. Different materials with pozzolanic properties such as fly ash, condensed silica fume, blast-furnace slag and rice-husk ash have played an important part in the production of high-performance concrete. Thousands of tonnes of these residues and industrial by-products are produced every year; therefore, the study of their characteristics and possible applications becomes a priority as their use brings benefits in technical, economic, power and environmental terms [12].

Among the different existing residues and by-products, the possibility of using rice-husk ash (RHA) has attracted more attention of cement researchers than other crop residues. First, due to the overabundance of this residue, 100 million tonnes of husk are obtained from an annual world production of 500 million tonnes of rice, a huge quantity of residue that can only be consumed by the cement and concrete industries that use a wide range of by-products according Mehta [13]. Secondly, rice-husk is not appropriate as feed for animals due to its few nutritional properties and its irregular abrasive surface is resistant to natural degradation, which poses serious accumulation problems. When it is incinerated, it produces a great quantity of

* Corresponding author. Tel.: +598 2711 7436; fax: +598 2711 7435.
E-mail address: gemma@fing.edu.uy (G.R. de Sensale).

0958-9465/$ - see front matter © 2007 Elsevier Ltd. All rights reserved.
doi:10.1016/j.cemconcomp.2007.04.005

ash. On average, each tonne of rice-husks, on complete combustion, produce 200 kg of RHA. No other crop residue generates a greater quantity of ash when it is burnt [13]. Thirdly, the use of RHA as a supplementary cementing material is of great interest to many developing countries where portland cement is in short supply but rice production is in abundance.

Fly ash, iron blast-furnace slag, condensed silica fume and RHA were identified for the 73-SBC RILEM Committee [14] as the principal by-products that possess pozzolanic and/or cementitious properties. It has been recognized that pozzolanic additions lead to important changes in fresh and hardened concrete, which depend on the mineral admixture type and content as well as on other mix components. A tremendous amount of literature is available on concrete containing pozzolanic materials [12], and different materials with pozzolanic properties such as fly ash, condensed silica fume and blast-furnace slag have played an important part in the production of high-performance concrete [15–18].

Pozzolanic additions reduce the porosity of concrete especially at the interfaces between cement paste and aggregates, which are the weakest zones of the material. The improvements produced by the mineral additions can modify the failure mechanism in concrete.

Recently, a study on the fracture characteristics of high-performance concrete was performed concluding that there is a reduction in the fracture energy due to the addition of fly ash and slag, attributed to the presence of unhydrated particles of size larger than that of normal flaws in concrete [19]. However, in this case mineral additions were included replacing 25% or 50% of the cement, and then a reduction in strength was also measured. That is not necessarily the situation when highly effective mineral additions such as silica fume replace part of the cement (usually no more than 10%).

The development and use of rice-husk ash (RHA) is not new [13]. Rice-husk ash is a mineral admixture for concrete [13,14], and much data has been published concerning its influence on the behaviour of concrete. Results for concretes with a 10% substitution of portland cement by RHA indicate excellent performance when compared to control concretes [20–26]. However, none of these studies investigated the effects of RHA on the failure mechanism of normal and high-strength concrete, including its influence on strength, stiffness, and fracture energy. As RHA is not commonly used in the production of HSC, this study is a contribution toward that goal. Specimens produced from several RHA concretes of differing water/binder ratios are tested in flexure and uniaxial compression. Analyses are made of the specimens response to these load conditions, with particular interest in the fracture properties of the material.

2. Experimental program

2.1. Materials and testing program

Four series of concretes with water/binder ratios (w/b) of 0.50, 0.40, 0.32 and 0.28 were made. Each series includes a concrete with 10% RHA as a cement replacement and a control concrete without RHA for comparison, according literature on concretes containing RHA [23,24]. Eight cylinders of 100×200 mm, four cylinders of 150×300 mm and eight beams of $105 \times 75 \times 430$ mm were cast in order to study the mechanical behaviour of each concrete.

Concretes were prepared using the following materials: natural siliceous river sand (fineness modulus of 2.43 and specific gravity of 2.63) as fine aggregate, crushed granite (maximum nominal size 20 mm and specific gravity of 2.65) as coarse aggregate, ordinary Portland cement, and rice-husk ash (RHA) dry-milled the necessary time to obtain a median particle size of 8 μm [22]. Table 1 shows the physical properties, chemical analysis, and activity index of the cement and the RHA. Strength measurements were performed on mortars, using prismatic specimens according UNIT 525 (similar to EN 196-1:1994).

A sulfonated naphthalene formaldehyde condensate-based superplasticizer (solids content 42%, specific gravity 1.20) was used, with the exception of NSC ($w/b = 0.50$).

The mixture proportions and the properties of fresh concrete are given in Table 2. NSC were designed to obtain a plastic consistency while in HSC the superplasticizer content was corrected to obtain a fluid concrete. The specimens were compacted by external vibration, varying the vibration time according to its consistency. They were kept protected after casting to avoid water evaporation, after

Table 1
Physical properties and chemical analyses of the cement and RHA used

	Cement	RHA
Physical tests		
Specific gravity	3.14	2.06
Fineness		
Specific surface, Blaine, m^2/kg	340.5	–
Nitrogen adsorption, m^2/kg	–	28.800
Setting time, min		
Initial	150	–
Final	230	–
Compressive strength, MPa		
1-day	18.8	–
3-day	48.7	–
7-day	55.4	–
28-day	58.5	–
Chemical analyses, (%)		
Silicon dioxide (SiO_2)	21.02	87.20
Aluminium oxide (Al_2O_3)	3.64	0.15
Ferric oxide (Fe_2O_3)	3.49	0.16
Calcium oxide (CaO)	64.59	0.55
Magnesium oxide (MgO)	0.74	0.35
Sodium oxide (Na_2O)	0.13	1.12
Potassium oxide (K_2O)	1.05	3.60
Loss on ignition	2.22	6.55
Activity index		
ASTM C311-98b	100	101

Table 2
Details of concrete mix proportions

Concrete	$w/(c+\text{RHA})$	RHA (%)	Cement (kg/m^3)	RHA (kg/m^3)	Fine aggregate (kg/m^3)	Coarse aggregate (kg/m^3)	Superplastizicer (%)	Slump (mm)
C-28	0.28	0	513	–	720	1005	2.00	170
RHA-28		10	468	34	730	1020	2.05	170
C-32	0.32	0	448	–	765	1005	1.20	180
RHA-32		10	401	29	765	1000	1.88	170
C-40	0.40	0	393	–	785	975	0.90	130
RHA-40		10	358	26	795	980	0.91	140
C-50	0.50	0	339	–	845	990	–	90
RHA-50		10	322	23	775	1045	–	80

24 h they were demoulded and stored in a moist room (21 ± 2 °C, 90–95% relative humidity) until testing age was achieved.

2.2. Test methods

Uniaxial compression tests were performed on cylinders of 150 × 300 mm and 100 × 200 mm. The 150 × 300 mm cylinders were made with the purpose of studying failure process under compressive loading through the analysis of the stress–strain curves. The axial and lateral deformations were monitored with LVDTs. Three loading–unloading cycles, up to 40% of the maximum stress, were applied to determine the modulus of elasticity and Poisson's ratio (ASTM C 469). After the third cycle the load was increased monotonically up to failure. Based on the stress–strain curves, the initiation (f_{init}) and critical (f_{crit}) stresses can be obtained, representing the starting of matrix crack growth and the onset of unstable propagation of cracks in the matrix of concrete [27,7]. The 100 × 200 mm cylinders were used to measure the compressive strength and modulus of elasticity, at 28 and 90 days.

Three-point bending tests of middle notched specimens were performed to study the stress–strain behaviour in tension, using beams of 105 mm height and 75 mm width. The notch was cut up to a depth equal to half of the beam's height and performed 1 day before testing using a diamond saw. A controlled closed loop system was used, the beams were loaded over a span of 400 mm and the tests were controlled by the average of the central deflection with a rate of 0.02 mm/min. In addition the crack mouth opening displacement at the notch (CMOD) was measured through a clip gage.

From the load–deflection curves, the net bending stress at maximum load (f_{net}), and the energy of fracture (G_F) from work-of fracture, were obtained following the general guidelines of the RILEM 50-FMC Committee [28]. The energy of fracture was calculated as $(W_0 + \text{mg}\delta_0)/A_{lig}$ where W_0 is the work-of fracture (equal to the area below the load–deflection plot), mg the contribution of the weight of the beam, δ_0 the displacement at the final fracture of the beam, and A_{lig} is the cross-sectional area of the ligament before the test. The net bending stress at maximum load was calculated as $f_{net} = 6\,(F_{max} + (\text{mg}/2))l/4bh^2$ where b is the width of the beam, h the depth of the ligament region above the prenotch, l the span and F_{max} is the maximum load. Finally, the characteristic length was calculated as $l_{ch} = EG_F/f_s^2$ using the values of the modulus of elasticity obtained from 100 × 200 mm cylinder tests and the splitting tensile strength (f_s) estimated as $0.6f_{net}$ [29,8]. Each result is the mean of four tests, both in the case of flexural or compressive tests.

3. Analysis of the results

3.1. Mechanical properties and failure mechanism in compression

Compression tests were performed at the age of 28 and 90 days on 100 × 200 mm cylinders to evaluate the evolution in compressive strength (f'_c) and modulus of elasticity (E) (see Table 3). Comparing control and RHA concretes, it can be clearly seen that f'_c increases in the later case, particularly for the lower w/b ratios. The relative compressive strength of RHA concretes increase to near 9 and 7% at 28 and 90 days, respectively. On the contrary, no significant changes in stiffness were observed (Fig. 1).

Table 3 also includes the results of compressive strength and modulus of elasticity obtained at 28 days on 150 × 300 mm specimens, which are consistent with those obtained on the smaller cylinders. Mean increments of the f'_c of RHA concretes were near 5% while the increase in modulus of elasticity was only 1% (see Fig. 2). It was also found that Poisson's ratio remains practically unaffected by RHA incorporation, although there is a slight increase. Comparing compressive strength of 100 × 200 mm and 150 × 300 mm cylinders, there is a mean increase of 9%, which is in accordance with general experience.

The failure mechanism of concrete in compression involves the growth and propagation of cracks, mainly through interfaces and matrix, and this process is reflected on the shape of the stress–strain curves of concrete [27].

More recently the same procedure was applied to analyse the failure mechanisms that take place in HSC [7].

Table 3
Compression tests

Specimens		Cylinders 100 × 200 mm				Cylinders 150 × 300 mm				
Testing age		28 days		90 days		28 days				
Concrete	RHA (%)	f'_c (MPa)	E (GPa)	f'_c (MPa)	E (GPa)	f'_c (MPa)	f_{crit} (%)	f_{init} (%)	E (GPa)	Poisson's ratio
C-28	0	69.5	40.5	74.3	43.8	63.1	98	96	40.9	0.199
RHA-28	10	74.9	42.4	82.1	42.9	63.6	>98	97	41.0	0.208
C-32	0	57.8	37.6	66.7	45.4	54.6	96	85	38.0	0.179
RHA-32	10	66.0	39.5	72.2	44.7	56.6	97	89	38.7	0.179
C-40	0	51.2	36.9	56.7	41.0	46.2	94	88	35.2	0.169
RHA-40	10	52.0	39.0	57.3	42.0	49.7	95	90	35.2	0.187
C-50	0	37.0	33.1	43.9	38.4	36.4	93	80	33.3	0.160
RHA-50	10	40.7	33.6	44.7	37.8	38.4	96	88	34.1	0.167

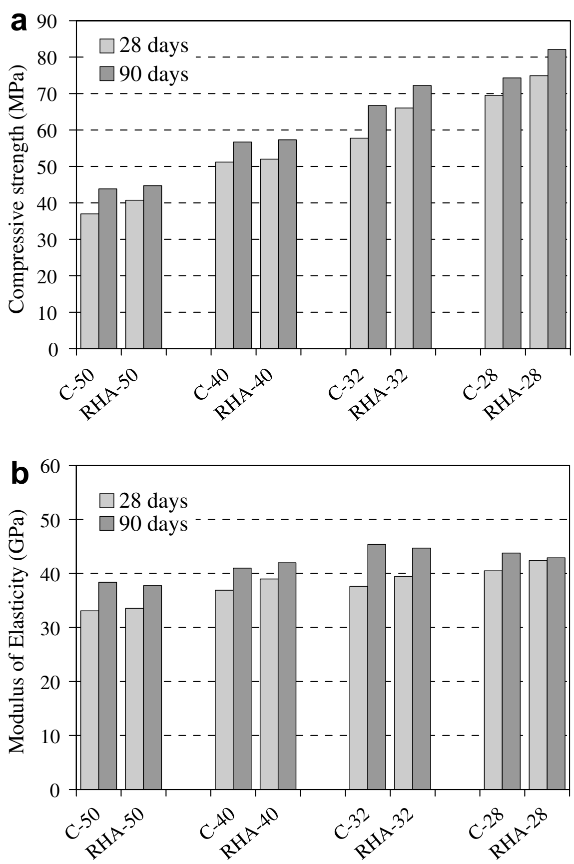

Fig. 1. Compressive strength (a) and modulus of elasticity (b) measured on 100 × 200 mm cylinders.

Stress vs. axial, lateral and volumetric strain curves of concretes were measured in tests performed at 28 days on 150 × 300 mm cylinders. As was mentioned above, two parameters can be obtained from the stress–strain curves, the initiation (f_{init}) and the critical (f_{crit}) stresses, which represent, respectively, the starting of matrix crack growth and the onset of unstable propagation of cracks in the matrix of concrete. Critical stress is defined as the stress corresponding to the minimum peak of strains in the volumetric strain

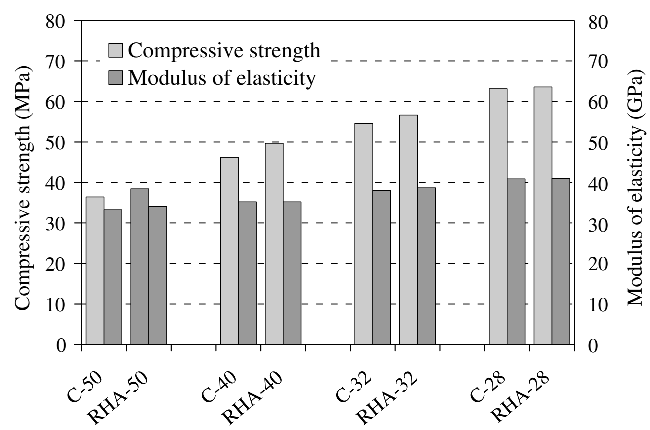

Fig. 2. Compressive strength and modulus of elasticity measured on 150 × 300 mm cylinders.

curve, while the initiation stress is obtained from stress vs. lateral/axial strain ratio curves as the stress at which this strain ratio clearly begins to increase.

Stress–strain curves are presented in Fig. 3. The results of initiation (f_{init}) and critical (f_{crit}) stresses, as a percentage of the compressive strength, are included in Table 3. As can be observed there were not significant differences in the shape of the curves corresponding to control and RHA concretes. Nevertheless, it must be noted that both f_{init} and f_{crit} increase in RHA concretes, indicating that the periods of stable and unstable crack propagation through the mortar matrix are reduced, showing a tendency to a more brittle failure mechanism. This fact is more evident when comparing the results in absolute values, as they are presented in Fig. 4. It appears that mortar cracks start growing at higher stresses and that the period of stable crack propagation (f_{crit}–f_{init}) tends to be reduced in RHA. However, it must be mentioned that the effect of RHA incorporation in the compressive failure mechanism of concrete is much smaller than that produced by a change in aggregate size [30] or the presence of cracks or other type of defects [31,32].

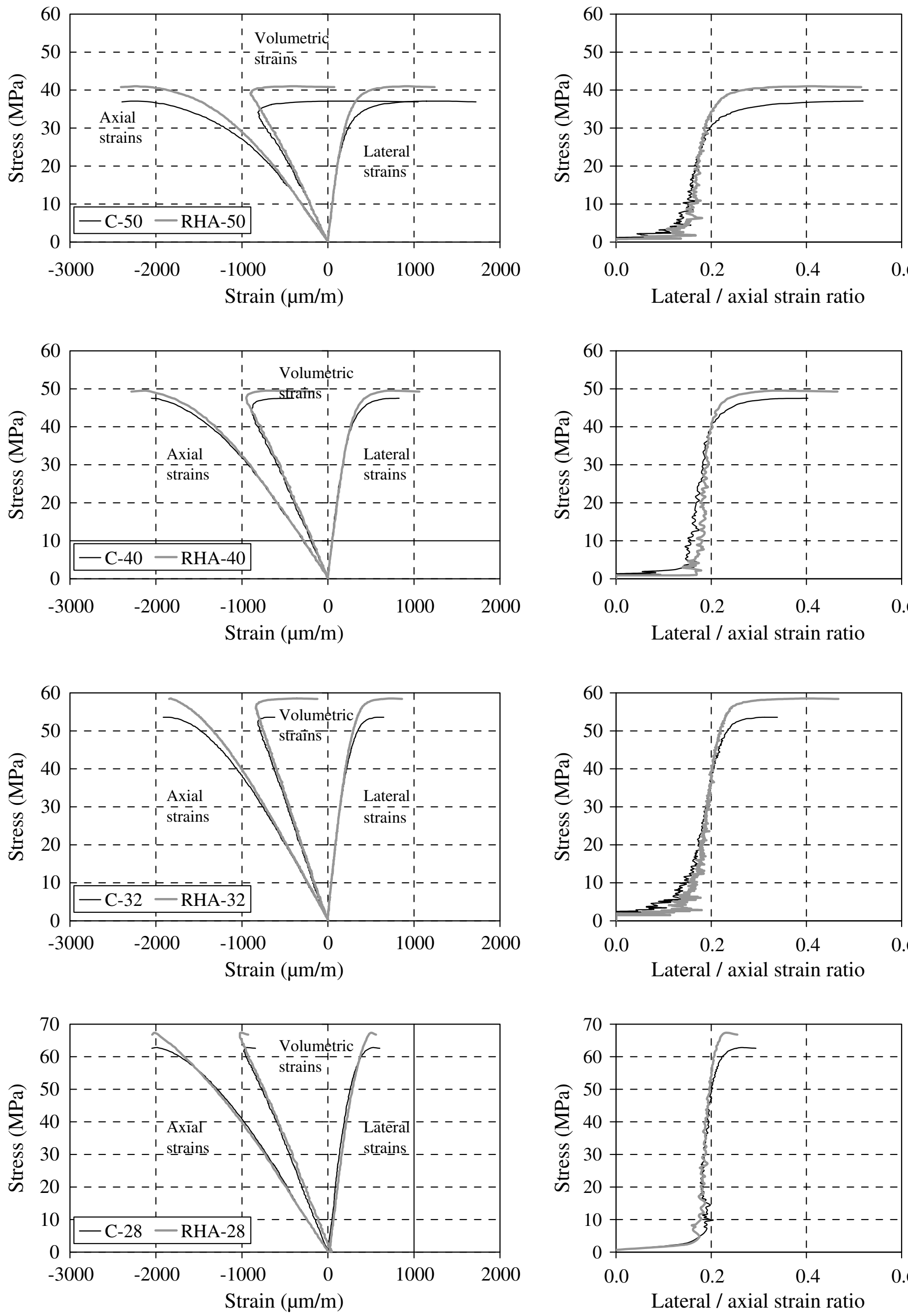

Fig. 3. Stress vs. axial, lateral and volumetric strain curves in compression (left). Stress vs. lateral/axial strain ratio curves (right).

3.2. Mechanical properties and failure mechanism in tension

Fracture tests are of special interest in the study of concrete failure mechanisms. Based on them, the effect of RHA incorporation on the flexural strength and the energy of fracture and the size of the fracture zone will be analysed.

Fig. 5 shows the typical load–deflection and load–CMOD curves, corresponding to RHA and control concretes with water/binder ratio 0.28 and 0.50. They were obtained from tests on centre-point loaded notched beams performed at the age of 90 days.

Table 4 presents the results of the net bending stress (f_{net}), the maximum deflection (δ_0) the energy of fracture (G_F), and the characteristic length (l_{ch}) obtained from the load–displacement curves at the ages of 28 and 90 days.

The response of concretes prepared with the same water/binder ratio and aggregate content, with and without RHA, was similar. The differences in the softening behaviour of concrete and then, the energy involved in the process of fracture, produced by the incorporation of RHA was smaller than those found changing the aggregate type and size and the relative strength levels between matrix and aggregates [6,8]. However, it was noted that in RHA

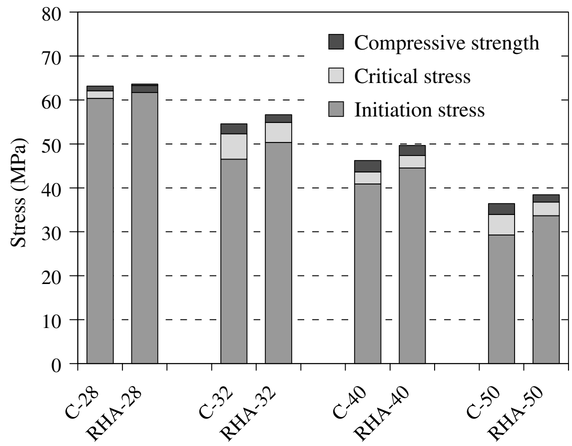

Fig. 4. Initiation and critical stresses and compressive strength in concretes with and without RHA.

concretes the softening branch of the curves were steeper and the maximum deflection were smaller than in control concretes.

With the aim to analyse the effect of RHA incorporation, Fig. 6. compares the results of the different series. It can be seen that when RHA was incorporated, although the flexural strength (f_{net}) tends to increase or remain equal (Fig. 6a) the energy of fracture (G_F) lightly decreases (Fig. 6b). This decrease in the energy of fracture (G_F) was observed both in normal strength and in HSC. As was expected, for the same concrete, the energy of fracture and the flexural strength increases with the age. Finally, the values of the characteristic length (l_{ch}) are compared in Fig. 6c. It must be indicated that l_{ch} is representative of the size of the fracture zone, and as l_{ch} decreases a more brittle behaviour appears, which is the situation of RHA concretes.

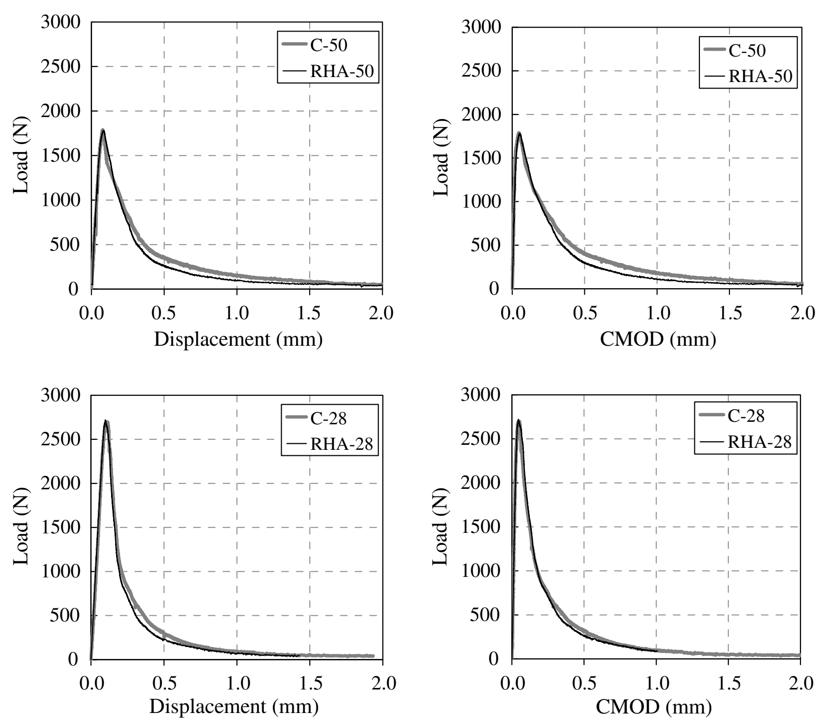

Fig. 5. Typical load–deflection and load–CMOD curves obtained from centre-point loading notched beams tested at the age of 90 days. ($w/b = 0.50$ and 0.28).

Table 4
Flexural tests

Concrete	RHA (%)	Testing age							
		28 days				90 days			
		f_{net} (MPa)	δ_0 (mm)	G_F (N/m)	l_{ch} (mm)	f_{net} (MPa)	δ_0 (mm)	G_F (N/m)	l_{ch} (mm)
C-28	0	7.6	1.3	180	350	8.0	2.0	205	390
RHA-28	10	7.6	1.4	180	365	7.6	1.9	185	380
C-32	0	5.8	1.9	185	575	6.8	2.0	215	580
RHA-32	10	6.1	1.4	165	485	7.2	1.7	200	475
C-40	0	5.1	1.8	175	690	5.8	2.2	205	695
RHA-40	10	5.0	1.5	155	670	5.3	1.6	165	685
C-50	0	4.0	1.7	140	805	5.1	2.0	180	740
RHA-50	10	4.5	1.3	125	585	5.2	2.2	175	680

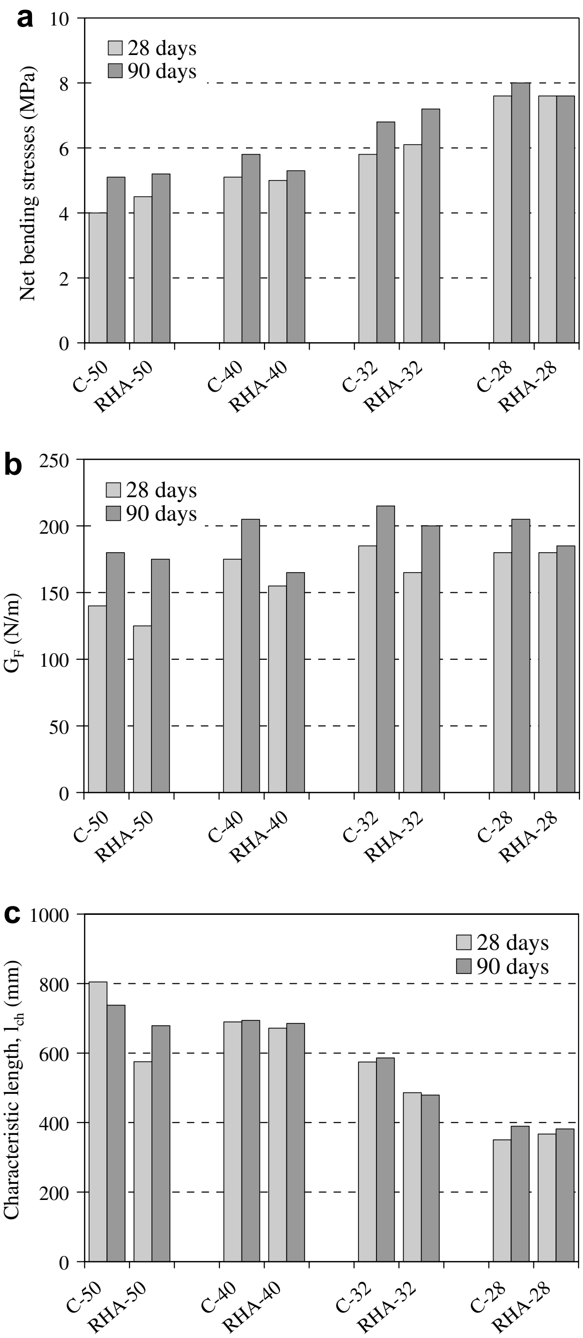

Fig. 6. Effect of RHA incorporation in flexural tests. (a) Flexural strength; (b) energy of fracture; (c) characteristic length.

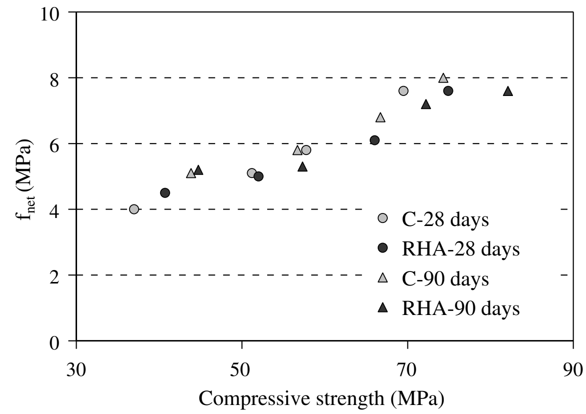

Fig. 7. Net bending stress vs. compressive strength.

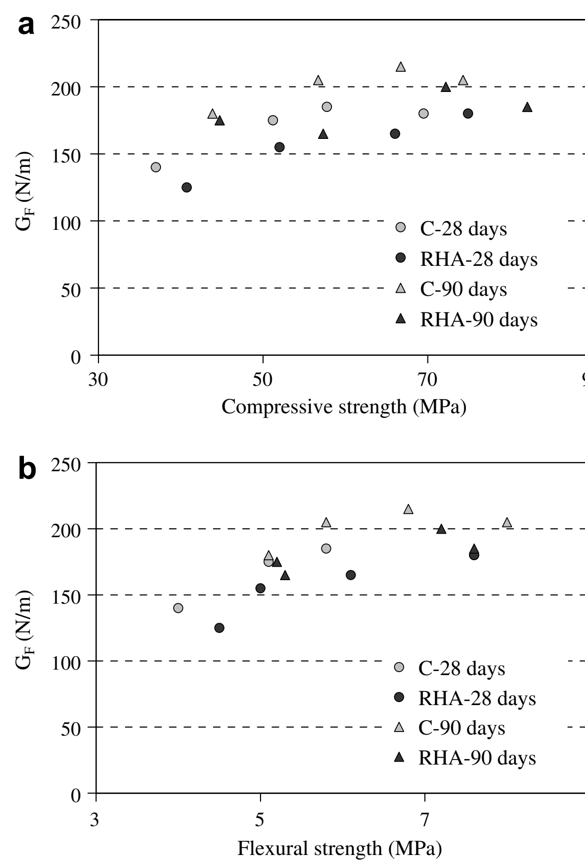

Fig. 8. Energy of fracture (G_F) vs. compressive (a) and flexural strength (b).

4. Discussion

From these experiences it appears that the replacement of 10% of cement by RHA enhances the mechanical strength (see Tables 3 and 4) with no significant effects on the flexural/compressive strength ratio (see Fig. 7). This was observed both in normal strength and in HSC, but it was particularly evident for the lower water/binder ratio concretes. Although peak loads are almost equal, flexural tests indicate a more brittle behaviour in RHA concretes, reflected by steeper softening curves than control concretes. This observation is consistent with other authors who found a decrease in the post-peak of the load–CMOD plot in fly ash and slag concretes compared with concrete without mineral additions [19]. The authors indicate that the more brittle failure occurs as a consequence of the densification of the concrete microstructure; however, in this case the strength also decreased. It must be noted that with the test geometry used both load–displacement and load–CMOD curves are very similar.

Fig. 8 shows the variation of the energy of fracture (G_F) with the compressive and the net bending strengths. Test

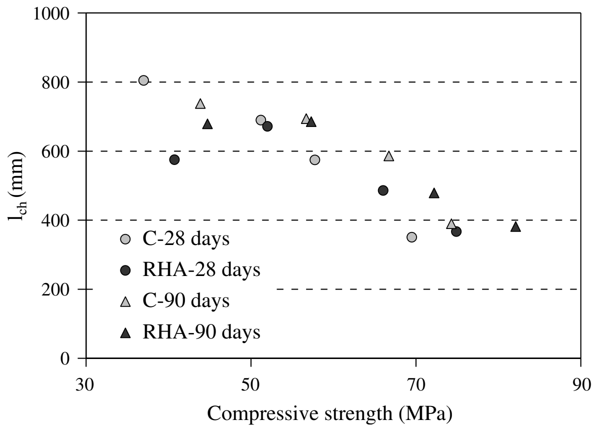

Fig. 9. Variation of the characteristic length with the compressive strength.

results obtained at 28 and 90 days are included. As it is known, the energy of fracture increases as strength increases even in HSC [9]. It can be clearly seen that for a same strength level points corresponding to RHA concretes are placed below those of the control concretes. Then, it appears that a relatively lower energy of fracture and a smaller increase in brittleness take place with the incorporation of RHA. This fact can be attributed to an improvement in the matrix–aggregate bond at interfaces and a reduction of defects in the internal structure of concrete. A similar behaviour has been observed in concretes with the addition of silica fume [33,34]. Finally, Fig. 9 presents the variation of the characteristic length with the compressive strength, showing that although RHA values tend to be placed slightly below the reference concrete ones, all follow a same pattern governed by the strength level.

It must be pointed that although there is a tendency to increase brittleness in RHA concretes (the energy of fracture was reduced to near 10%), this percentage is much smaller than the variations that may be produced by a change in the type [6,9] or size of coarse aggregate [29]. In most cases, it is likely that improvements in the durability of concrete structures due to the reduction in porosity and densification of the microstructure will be more significant than the observed effect of increasing the relative brittleness of the concrete.

5. Conclusions

This paper analyses the failure behaviour in tension and in compression of normal and high-strength concretes with and without optimised rice-husk ash (RHA). The main conclusions are as follows:

The incorporation of RHA in concretes produced increases in compressive strength, particularly for the lower water/binder ratio concretes, and no significant changes in the modulus of elasticity and in the Poisson's ratio. The analysis of the failure mechanism in compression indicates that the stresses at which cracks initiate and propagate are higher in RHA concretes, so that there is a tendency for more brittle failure mechanisms.

Flexural tests also make evident that the use of RHA produced a small increase in brittleness. While the flexural strength remained equal or increased, the energy of fracture slightly decreased. Comparing concretes with and without RHA a decrease in characteristic length also appeared. This behaviour was observed both in normal strength and in high-strength concrete. However, it must be pointed that for the same strength level, the energy of fracture was reduced no more than 10%, which is much smaller than the variations that may be produced by a change in the type or size of coarse aggregate.

References

[1] ACI Committee 363. State-of-art report on high-strength concrete (ACI 363.R-92/97). In: Manual of concrete practice ACI; 1998. 55 pp.
[2] Tasdemir C, Tasdemir M, Mills N, Barr BIG, Lyndon FD. Combined effects of silica fume, aggregate type, and size post-peak response of concrete in bending. ACI Mater J 1999;96(1):74–83.
[3] Gettu R, Bazant ZP, Martha EK. Fracture properties and brittleness of high strength concrete. ACI Mater J 1990;87(6):608–18.
[4] Rao GA, Raghu Prasad BK. Size effect and fracture properties of HPC. In: Proceedings of the 14th engineering mechanics international conference (ASCE); 2000. p. 21–4.
[5] Rao GA, Raghu Prasad BK. Fracture energy and softening behaviour of high strength concrete. Cem Concr Res 2002;32:247–52.
[6] Giaccio G, Zerbino R. Failure mechanism of concrete: combined effects of coarse aggregates and strength level. Adv Cem Based Mater 1998;7(1):41–8.
[7] Giaccio G, Rocco C, Violini D, Zappitelli J, Zerbino R. High strength concretes incorporating different coarse aggregates. ACI Mater J 1992;89(3):242–6.
[8] García-Alvarez VO, Giaccio G, Zerbino R, Gettu R. Influence of the nature of the aggregate on the cracking mechanisms of normal and high strength concrete. Cemento-Hormigón 2003;857:40–54 [only available in spanish].
[9] Giaccio G, Rocco C, Zerbino R. The fracture energy (G_F) of high-strength concretes. Mater Struct 1993;26(161):381–6.
[10] Zhou FP, Barr BIG, Lydon FD. Fracture properties of high strength concrete with varying silica fume content and aggregates. Cem Concr Res 1995;25(3):543–52.
[11] Gopalakrishnan S, Balasubramanian K, Krishnamoorthy TS, Bharatkumar BH. Investigations on reinforced high performance beams. In: ACI, vol. SP-199; 2001. p. 645–63.
[12] Malhotra VM, Mehta PK. Pozzolanic and cementitious materials. Advances in concrete technology, vol. 1. Canada: Gordon and Breach Publishing; 1996.
[13] Mehta PK. Rice husk ash – a unique supplementary cementing material. In: Proceedings of the CANMET/ACI international conference on advances in concrete technology. Canada: CANMET; 1992. p. 419–43.
[14] RILEM Committee 73-SBC. Final report: siliceous by-products for use in concrete. Mater Struct 1988;21(121):69–80.
[15] Mehta PK. Role of pozzolanic and cementitious materials in sustainable development of the concrete industry. In: ACI, vol. SP-179; 1998. p. 1–20.
[16] Krishnamoorthy TS, Gopalakrishnan S, Balasubramanian K, Bharatkumar BH, Rama Moan Rao P. Investigations on the cementitious grout containing supplementary cementitious materials. Cem Concr Res 2002;32(9):1345–405.
[17] Swamy RN. Design for durability and strength through the use of fly ash and slag in concrete. In: ACI, vol. SP-171; 1997. p. 1–72.

[18] Mehta PK. Concrete technology at the cross-roads-problems and opportunities. In: ACI, vol. SP-144; 1994. p. 1–30.
[19] Bharatkumar BH, Raghuprasad BK, Ramachandramurthy DS, Narayanan R, Gopalakrishnan S. Effect of fly ash and slag on the fracture characteristics of high performance concrete. Mater Struct 2005;38(275):63–72.
[20] Mehta PK, Pitt N. A new process of rice husk utilization. In: International conference on the utilization of rice by-products, 1974. Valencia: IATA; 1977. p. 45–58.
[21] James J, Rao MS. Reactivity of rice husk ash. Cem Concr Res 1986;16:296–302.
[22] Mehta PK. Highly durable cement products containing siliceous ashes. US Patent 5,346,548; 1994. 15 pp.
[23] Zhang MH, Lastra R, Malhotra VM. Rice-husk ash past and concrete: some aspects of hydration and the microstructure of the interfacial zone between the aggregate and paste. Cem Concr Res 1996;26(6):963–77.
[24] Zhang MH, Malhotra VM. High-performance concrete incorporating RHA as a supplementary cementing material. ACI Mater J 1996;93(6):629–36.
[25] de Sensale GR, Dal Molin DCC. Study of high performance concrete, regarding the effects of rice-husk ash substitution. In: Precast/Prestressed Concrete Institute, editor. Proceedings of the PCI/FHWA/FIB international symposium on high performance concrete; 2000. p. 135–44.
[26] de Sensale GR. Strength development of concrete with rice-husk ash. Cem Concr Compos 2006;28(2):158–60.
[27] Shah SP, Chandra S. Critical stress, volume change, and microcracking of concrete. ACI Mater J 1968;65(9):770–81.
[28] RILEM TC-50 FMC. Determination of the fracture energy of mortar and concrete by means of three-point bend tests on notched beams. Mater Struct 1985;18(106):285–90.
[29] Hillerborg A. Additional concrete fracture energy test performed by 6 laboratories according to a draft RILEM recommendation. Report TVBM-3017. Division of Building Materials, Lund Institute of Technology; 1984. 12 pp.
[30] Di Maio A, Giaccio G, Zerbino R. Failure mechanism of concrete, combined effects of coarse aggregate and specimen geometry. Construct Build Mater 1997;10(8):571–5.
[31] Barragán B, Di Maio A, Giaccio G, Traversa L, Zerbino R. Effects of high temperature on residual, mechanical, and transport properties of concrete. In: Malhotra VM, editor. Proceedings of the fifth CANMET/ACI international conference on durability of concrete, vol. ACI SP-192; 2000. p. 983–1000.
[32] Batic O, Giaccio G, Zerbino R. On the effect of ASR cracking on the mechanical behaviour of concrete in tension and compression. In: Tang M, Deng M, editors. Int. Acad. Publishers, World Pub. Corp., vol. 2. ISBN: 7-5062-7033-1; 2004. p. 1136–41.
[33] Gettu R, Garcia-Álvarez VO, Aguado A. Effect of aging on the fracture characteristics and brittleness of a high-strength concrete. Cem Concr Res 1998;28(3):349–55.
[34] Tasdemir C, Tasdemir MA, Lydon FD, Barr BIG. Effects of silica fume and aggregate size on the brittleness of concrete. Cem Concr Res 1996;26(1):63–8.